

**MODELLING OF SHOCK WAVE IN CONVERGING-DIVERGING
NOZZLE USING SHOCK CAPTURING METHOD**

BY

MOHD NAZARUDIN BIN ROSLI

**DISSERTATION SUBMITTED IN PARTIAL FULFILMENT OF
THE REQUIREMENTS FOR THE
BACHELOR OF ENGINEERING (HONS)
(CHEMICAL ENGINEERING)**

JANUARY 2010

**UNIVERSITI TEKNOLOGI PETRONAS
BANDAR SERI ISKANDAR
31750 TRONOH L RIDZUAN**

CERTIFICATION OF APPROVAL

**MODELLING OF SHOCK WAVE IN CONVERGING-DIVERGING NOZZLE
USING SHOCK CAPTURING METHOD**

by

Mohd Nazarudin bin Rosli

(8485)

A project dissertation submitted to the

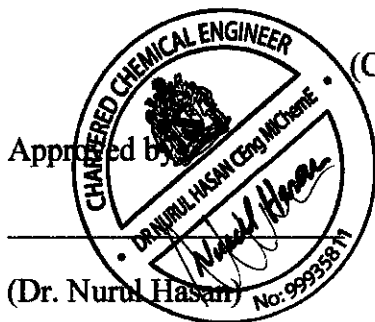
Chemical Engineering Programme

Universiti Teknologi PETRONAS

in partial fulfilment of the requirement for the

BACHELOR OF ENGINEERING (Hons)

(CHEMICAL ENGINEERING)



UNIVERSITI TEKNOLOGI PETRONAS

TRONOH, PERAK

January 2010

CERTIFICATION OF ORIGINALITY

This is to certify that I am responsible for the work submitted in this project, that the original work is my own except as specified in the references and acknowledgements, and that the original work contained herein have not been undertaken or done by unspecified sources or persons.



13/6

Mohd Nazarudin bin Rosli (8485)

ACKNOWLEDGEMENT

The acknowledgement is primarily dedicated to my final year project supervisor, Dr Nurul Hasan, who has worked so hard to ensure that we will get the necessary knowledge and skills to complete our projects. Through Dr Nurul, I was introduced to varieties of computational fluid dynamics (CFD) simulation softwares such as ANSYS FLUENT 12.0, ANSYS CFX 12.0, COMSOL Multiphysics, and GAMBIT 2.4.6. It is very hard to find a dedicated and encouraging supervisor like Dr Nurul Hasan. I am in great debt to him; hopefully I will have the opportunity to pay him back for his knowledge and moral support, and all the advice and experience he shared throughout the period of working together.

Not to forget, many thanks to my colleague, Zalinawati bt Zakaria, and also postgraduate student under Dr Nurul, Mr Dang Dinh Thang. They have given me the moral support as well as sharing knowledge – all the components needed for me to keep moving forward in going through my FYP. Thanks so much again guys. Hope we will meet again as CFD practitioners after graduation.

The project is definitely an eye opener to the possibilities of using CFD for intensive research in process intensification, a new area of chemical engineering. Since the project is utilizing converging-diverging nozzle and involve thorough study of supersonic gas flow, an area which usually of concern to rocket science, I am very amazed at how much improvement it could make to process equipments. It clearly shows that if we would take the time to analyse the research area from other fields, we might stump into the solution that we are looking for.

TABLE OF CONTENTS

| Section | Page |
|---------------------------|-------------|
| Abstract | 6 |
| List of Table | 7 |
| List of Figure | 7 |
| List of Nomenclature | 8 |
| 1.0 Introduction | 9 |
| 1.1 Background of study | 9 |
| 1.2 Problem statement | 9 |
| 1.3 Objective of study | 11 |
| 1.4 Scope of study | 11 |
| 2.0 Literature Review | 12 |
| 3.0 Methodology | 19 |
| 3.1 Grid development | 19 |
| 3.2 Simulation setup | 22 |
| 3.3 Grid refinement study | 25 |
| 3.4 Data visualisation | 27 |
| 4.0 Result and Discussion | 28 |
| 4.1 Grid Refinement | 29 |

| | | |
|---------|--|----|
| 4.1.1 | Effect of Grid Density | 30 |
| 4.1.2 | Effect of Grid Refinement Direction | 32 |
| 4.1.2.1 | Axial Refinement | 32 |
| 4.1.2.2 | Radial Refinement | 32 |
| 4.1.2.3 | Axial-Radial Refinement | 33 |
| 4.1.3 | Small and large NPRs result comparison | 36 |
| 4.2 | Shock Structure Evaluation | 38 |
| 5.0 | Conclusion and Recommendation | 42 |
| 5.1 | Conclusion | 42 |
| 5.2 | Recommendation | 43 |
| 6.0 | Reference | 44 |
| 7.0 | Appendices | 45 |
| 7.1 | Gantt Chart of FYP I | 45 |
| 7.2 | Gantt Chart of FYP II | 46 |

Modelling of Shock Wave in Converging-Diverging Nozzle using Shock Capturing Method

Mohd Nazarudin bin Rosli and Dr Nurul Hasan*,
Dept Chemical Eng, Universiti Teknologi PETRONAS,
Bandar Seri Iskandar, 31750 Tronoh, Perak Darul Ridzuan, Malaysia

Abstract:

The formation of shock has always seen as undesirable occurrence. The knowledge about its formation is critical especially during design stage. Highly accurate numerical model are needed in order to accurately simulate formation of shock. One case study on supersonic flow separation has been selected as basis. Grid independent study is done to study the effect of grid density as well as refinement direction (axial, radial, and both axial and radial) to the accuracy of the solution. It is also desirable to investigate the formation of shocks under different nozzle operating pressures. The simulation is using several nozzle pressure ratios (NPRs) as manipulated parameters. Simulation results show that refinement in radial direction gives the optimum trend following data while refinement in both axial and radial gives quite accurate data but not following the experimental data trend. Higher density mesh is found to be capable of capturing weak shocks and shock-boundary layer interaction. Lastly, under different operating pressure, it is found that shocks location is closer to the throat as the nozzle pressure ratio is decreased.

Keywords: Shock Wave, Flow Separation, Nozzle Pressure Ratio. Grid Refinement

*Dr Nurul Hasan
Universiti Teknologi PETRONAS,
Bandar Seri Iskandar, 31750 Tronoh, Perak Darul Ridzuan, Malaysia
Nurul_hasan@petronas.com.my

List of Table

| | | |
|------|--|----|
| 3.1: | List of nozzle pressure ratio used for investigation..... | 22 |
| 3.2: | Experimental shock pressures and shock locations under different NPRs.... | 24 |
| 3.3: | List of meshes with cell and face size..... | 25 |
| 4.1: | Predicted shock pressure and shock location of nozzle topwall, and deviation from experimental values..... | 35 |

List of Figure

| | | |
|------|---|----|
| 2.1: | Shock structure in overexpanded condition a) Inviscid fluid, b) Viscous fluid with separated boundary layer..... | 13 |
| 2.2: | Anatomy of converging-diverging nozzle..... | 14 |
| 3.1: | Nozzle setup used for experiment in Mixing Enhancement of Axial Flow and Supersonic Flow Separation in Planar Nozzle by Papamouschou et all (2008)..... | 19 |
| 3.2: | Computational domain for the simulation a) Full view, b) Zoom view into converging-diverging nozzle section..... | 21 |
| 3.3: | Schlieren image of nozzle plume. Taken from Mixing Enhancement studies by Papamouschou (2000)..... | 23 |
| 3.4: | Experimental data of pressure distribution at nozzle topwall, taken from supersonic flow separation studies by Papamouschou et all (2008)..... | 24 |
| 3.5: | Mesh after refinement in three different directions, a) Axial, b) Radial, c) Axial – Radial..... | 26 |
| 4.1: | Centreline pressure distributions of original mesh..... | 29 |
| 4.2: | NPR 1.27 pressure distributions on different grid refinement direction at a) Centreline Section, b) Topwall Section..... | 30 |
| 4.3: | Nozzle pressure distributions at nozzle centerline (CL) and topwall (TW) using axial 1, radial 1, and axi-radi 1 mesh..... | 34 |
| 4.4: | Comparison of pressure distribution between small and large NPR values. Refinement direction a) Axial, b) Radial, c) Axial-Radial..... | 37 |
| 4.5: | Flow pattern of NPR 1.27 condition inside the nozzle from three different meshes a) Axial 2, b) Radial 2, c) Axial-Radial 2..... | 39 |
| 4.6: | Contour of velocity magnitude a) Axial 2, b) Radial 2, c) Axi-Radi 2..... | 40 |

List of Nomenclature

- A = Nozzle cross-sectional area
- E = Internal energy
- H = Nozzle height
- h = Enthalpy
- Ma = Mach number
- NPR = Nozzle pressure ratio, Stagnation pressure/Ambient pressure (P_0/P_{amb})
- P = Pressure
- P_0 = Total pressure at nozzle inlet
- R = Gas constant
- T = Temperature
- u,v,w = Velocity components
- x = Axial direction
- y = Normal direction
- γ = ratio of specific heats
- μ = Viscosity

Subscripts:

- 0 = total
- 1 = immediately before the Mach stem
- 2 = immediately after the Mach stem
- a = ambient
- c = centreline
- e = nozzle exit
- s = shock location
- t = throat

CHAPTER 1:

INTRODUCTION

1.1 Background of Study

Converging-diverging (CD) nozzle (or Laval nozzle) is one of the most important engineering hardware. It is used in many types of equipment covering a wide range of industrial applications. The primary function of CD nozzle is to accelerate the gas flow to supersonic speed. Whenever supersonic flow is concern, a phenomenon called shock wave will appear as a result of sudden change of fluid properties such as pressure, temperature, and density. Different operating condition of the nozzle will affect the formation and the shape of shock wave in many ways.

Theoretically, under the drive for process intensification, it is believed that many process equipments can be modified for smaller size and better efficiency while maintaining or increasing the throughput. One of the components suggested for use is converging-diverging nozzle. This has lead to increasing interest in applying converging-diverging nozzle in chemical engineering system as well as the need for deeper understanding of converging-diverging nozzle and supersonic flow.

In this paper, the research will be focusing on the modelling of shock wave in converging-diverging nozzle using a numerical technique called Shock Capturing Method (SCM). The results of the research will reveal the factors affecting the accuracy of Shock Capturing Method and the dynamics of shock pattern under different operating conditions. Later, it will be a step stone to further understanding the behaviour of shock wave in converging-diverging nozzle.

1.2 Problem Statement

Shock wave in general is a phenomenon that creates sudden change of fluid properties across the shock wave. The phenomenon, however, possesses the ability to interact with other fluid structures such as boundary layer. Interaction of shock wave with boundary layer will eventually reaches a point where the boundary layer start to

separate - a phenomenon called supersonic flow separation. The interaction will cause unwanted oscillation to the solid structure which will reduce the life span of equipment. The effect of shock wave is crucial during the design stage of various supersonic devices such as gas turbine and nozzle, to name a few. Extensive research has been done to find the suitable method of designing shock free supersonic device and to successfully achieve that stage, scientists and engineers will need to understand the shock wave dynamic.

Certain chemical process requirement desire extreme changes in process condition in order to maximize efficiency. Example of such processes is Rapid Quenching of Magnesium and Carbon Monoxide vapor, which need to be done within short period of time to avoid reversible reaction [1]. Within process engineering practitioner, the interest to utilize the properties dynamics of converging-diverging nozzle is increasing. Another interest is on fluid mixing enhancement that occurs in converging-diverging nozzle at supersonic speed. The mixing is expected to able to efficiently mixed flows without the use of mechanical mixers and it is also mixing in linear flow, unlike current practice that utilized flows from different direction for mixing [2].

To accomplish all the cases above, the scientific community needs to understand the behaviour of compressible flow in converging-diverging nozzle. Most importantly, the basic of such flow which are formation of shock and prediction of shock location under different operating conditions are highly crucial. Normally, researchers will conduct experiments to analyse the flow. However, the cost of running experiments at the level of supersonic and hypersonic speed is very expensive that it requires millions of dollars.

Therefore, Computational Fluid Dynamics (CFD) modelling is seen as the best and cost effective solution. Thus, the requirement above arise the need to develop mathematical models which can accurately simulate the formation of shock wave in various operating condition.

1.3 Objective of Study

1. To simulate the formation of shock wave in converging-diverging nozzle using Shock Capturing Method
2. To investigate the effect of mesh refinement to the accuracy of solution
3. To investigate the formation of shocks under different nozzle operating pressures

1.4 Scope of Study

The modelling will focus on two dimensional axisymmetric compressible flow. It will cover the parameters affecting the formation of shock wave in converging-diverging nozzle. As a start, thorough study will be done with the latest advancement in the area especially on the application of Shock Capturing Method on supersonic flow.

CHAPTER 2:

LITERATURE REVIEW

The advance of Computational Fluid Dynamics (CFD) research has lead to numerous developments in understanding the behavior of shock, the application of converging-diverging nozzle, as well as improvement of Shock Capturing Method. Currently scientist and engineers are researching to understand interacting factors that could affect shock wave.

A compressible fluid is known to display interesting characteristics and features along with the change of fluid properties and operating parameters. One of it is formation of shock, a phenomenon which forms whenever the flow reaches supersonic speed, $Ma > 1.0$. Physically, shock forms as a result of spontaneous release of energy, which leads to sharp change in fluid properties. By numerical definition, it is represented by discontinuity of solution of mass, momentum, and energy equations.

Formation of shock wave is caused by propagation of disturbance moves in supersonic speed within region of compressible fluid. Compression wave is created by the high speed movement of disturbance. Depending on different fluid region and disturbance properties, shock wave will form in different shapes and locations. In term of thermodynamics, the presence of shock wave increases entropy within the region. Eventually, due to the high positive entropy, the shock wave will degenerated spontaneously as an effect of dissipation of energy to the environment. Normal shock wave, as seen in Figure 2.1, is the simplest type of shock, often use as assumption to simplify compressible flow computation.

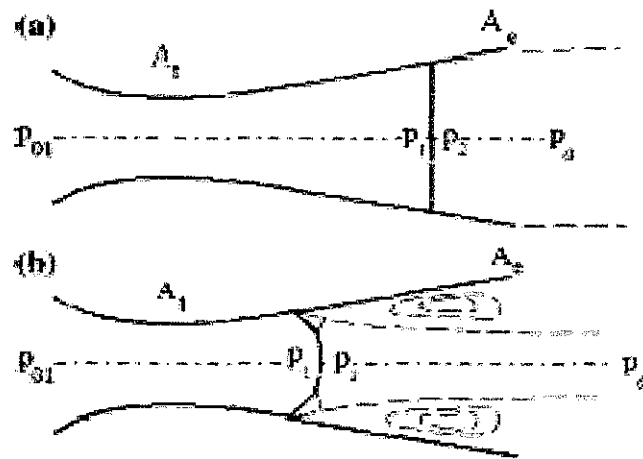


Figure 2.1: Shock structure in overexpanded condition [3]

a) Inviscid fluid, b) Viscous fluid with separated boundary layer

Shock can occur externally and internally, depending on the equipments used. External flow shock is mostly observed at bodies moving at supersonic and hypersonic speed. Well known examples are high speed jet and space rocket. Shock can be seen to form on top of the jet and rocket solid structures. Different from external flow, shock form from internal flow is much harder to observe as it usually take place in equipments such high pressure gas pipelines, and in many turbo-machineries such as compressors and turbo-expanders.

For an internal flow to reach supersonic speed, it needs to fulfil certain conditions together with the use of special piece of device. The only device capable of accelerating a gas flow to supersonic and hypersonic speed is called converging-diverging nozzle, or better known as de Laval nozzle. This interesting characteristic is contributed by unique geometry of the nozzle. Referring to Figure 2.2, it is a combination of converging part (a normal nozzle) and diverging part (a diffuser).

There are, however, specific operating conditions that needs to be fulfilled for the acceleration will take place – the back pressure (the ambient pressure after the nozzle outlet) need to be low enough. Under the influence of different nozzle pressure ratio, variation of shock shapes and structure will form inside the nozzle [4]. Extensive research has been done to find the best method to produce shock free nozzle and to obtain full understanding of shock phenomena.

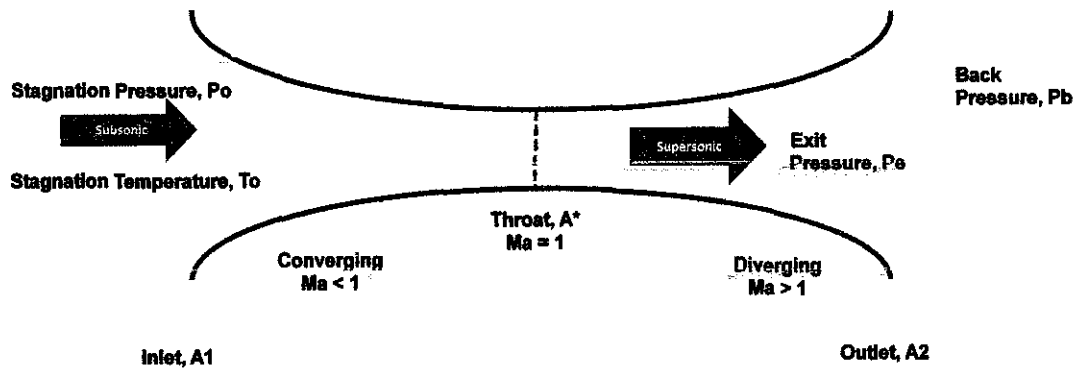


Figure 2.2: Anatomy of converging-diverging nozzle

Applying thermodynamics theories to converging-diverging nozzle, three most important parameters which are area, temperature, and pressure can be computed by solving the quasi 1-D equations as below (Anderson, 2000). The equations are represented by non-dimensional ratio of each parameter.

Equation 1 – Nozzle temperature ratio (NTR)

$$\frac{T}{T_0} = \left[1 + \left(\frac{\gamma - 1}{2} \right) M^2 \right]^{-1} \dots \dots \dots (1)$$

Equation 2 – Nozzle pressure ratio (NPR)

$$\frac{p}{p_0} = \left[1 + \left(\frac{\gamma - 1}{2} \right) M^2 \right]^{\frac{\gamma}{\gamma - 1}} \dots \dots \dots (2)$$

Equation 3 – Nozzle area ratio (NAR)

$$\frac{A}{A^*} = \frac{1}{M} \left[1 + \left(\frac{\gamma - 1}{2} \right) m^2 \right]^{-1} \dots \dots \dots (3)$$

Shock is known to be a very unstable structure. Due to the high energy content, shock display high degree of instability. It induces vibration to the solid structure during its interaction with boundary layer, and eventually reduces the lifespan of the structure/equipment. Numerous efforts are done to counter this problem. One of the studies conducted is to find a way to minimised the effect of shock induced vibration. Researchers discovered that at certain inlet pressure fluctuation frequencies, the vibration magnitude is reduced [5]. Overall, highlighted by Papamouschou (2000), one of most important factor to ensure successful numerical simulation of shock mixing is to accurately locate the shock.

Apart from the undesirable effects, interaction of shock with boundary layer within converging-diverging nozzle also known to produce interesting features. The separation of supersonic flow induces mixing effect, which in turn has great potential as linear fluid mixer [6]. Extensive research is currently done in academia to understand the properties of supersonic fluid mixing. Numerical [3] and experimental [7] work suggested that supersonic mixing is possible provided the correct nozzle pressure ratio (NPR) is used to create the desired shock.

The rapid change in fluid properties caused by shock is becoming increasingly important in the engineering community including in chemical engineering. In the field of mineral processing, rapid quenching of magnesium vapour and carbon monoxide is achieved by manipulating the sudden decrease in temperature inside converging-diverging nozzle [8]. In another case, converging-diverging nozzle is also used in case of condensing steam. Numerical investigation of the condensing steam in converging-diverging nozzle has been done recently [9].

Indeed, the greatest obstacle to achieve the best shock simulation is to accurately find the shock location inside the nozzle [10]. There are two most prominent techniques in modelling shock waves, which are Shock Capture and Shock Fitting techniques [11]. Shock Capture works by directly solving Navier-Stokes equations and shock will form as part of the solution. Due to its flexibility and ability to handle complex multidimensional flow, Shock Capturing Method is always preferred than Shock Fitting Method. This technique is the main focus of the paper.

The presence of shock is represented by sharp discontinuities of solution within the computational domain. However, a problem arises when the solution tends to oscillate. The oscillation leads to inaccuracy of the result [12]. Several methods have been proposed to overcome the problem; one of them is artificial viscosity. By imitating the function of viscosity term in Navier-Stokes equations, an additional term is added to the equation. The value of the additional terms is observed to reduce oscillatory behaviour of solution by smearing the solution. This term is artificial viscosity. A recent method developed to combine with artificial viscosity is Discontinuous Galerkin Method [13].

Despite the ability to reduce oscillation, excessive use of artificial viscosity, however, reduces the accuracy of the solution since it promotes smearing of solution

Apart from the undesirable effects, interaction of shock with boundary layer within converging-diverging nozzle also known to produces interesting feature. The separation of supersonic flow induces mixing effect, which in turn have great potential as linear fluid mixer [6]. Extensive research is currently done in academia to understanding the properties of supersonic fluid mixing. Numerical [3] and experimental [7] work suggested that supersonic mixing is possible provided the correct nozzle pressure ratio (NPR) is used to create the desired shock.

The rapid change in fluid properties caused by shock is becoming increasingly important in engineering community including in chemical engineering. In the field of mineral processing, rapid quenching of magnesium vapour and carbon monoxide is achieved by manipulating the sudden decrease in temperature inside converging-diverging nozzle [8]. In another case, converging-diverging nozzle is also used in case of condensing steam. Numerical investigation of the condensing steam in converging-diverging nozzle has been done recently [9].

Indeed, the greatest obstacle to achieve the best shock simulation is to accurately find the shock location inside the nozzle [10]. There are two most prominent technique in modelling shock wave, which are Shock Capture and Shock Fitting technique [11]. Shock Capture works by directly solving Navier-Stokes equation and shock will form as part of the solution. Due to its flexibility and ability to handle complex multidimensional flow, Shock Capturing Method is always preferred than Shock Fitting Method. This technique is the main focus of the paper.

The presence of shock is represented by sharp discontinuities of solution within the computational domain. However, problem arises when the solution tend to oscillate. The oscillation leads to inaccuracy of the result [12]. Several methods have been proposed to overcome the problem; one of it is artificial viscosity. By imitating the function of viscosity term in Navier-Stokes equation, an additional term is added to the equation. The value of the additional terms is observed to reduce oscillatory behaviour of solution by smearing the solution. This term is artificial viscosity. A recent method developed to combine with artificial viscosity is Discontinuous Galerkin Method [13].

Despite the ability to reduce oscillation, excessive use of artificial viscosity, however, reduces the accuracy of the solution since it promotes smearing of solution

over several grids. Recently, advance algorithm has take place by combining the artificial viscosity methods with Total Variation Diminishing (TVD) and Weighted Essentially Non-Oscillatory (WENO) schemes [14]. The schemes are found to be capable of recovering the accuracy of information of the shock discontinuities.

Up till now, it can be seen that the greatest problem regarding shock modelling is to accurately locate the shock. The most prominent and accurate numerical schemes are the use of TVD and WENO combined with artificial viscosity, whereby artificial viscosity works as stabilizer and WENO works to recover the accuracy information lost during the computation.

As mentioned previously, Shock Capturing works by directly solve the set of mass and momentum (Navier-Stokes equation) and energy equations. For multidimensional flow, solving will require great amount of computational power. Due to processing capability limitations, scientists and engineers always try to model complex fluid flow phenomena with simpler models. In many cases, Navier-Stokes equation is simplified by averaging the time-dependent components, converting it into what we call now as Reynolds-Average Navier-Stokes (RANS) equation as shown by the following set of continuity and momentum equation. These two equations are the primary physical models used for the simulation.

Since the scope of study of the research is in 2D-axisymmetry, the computational domain of nozzle will follow suit. Thus, the following continuity equation is used:

$$\frac{\partial \rho}{\partial t} + \frac{\partial}{\partial x}(\rho v_x) + \frac{\partial}{\partial r}(\rho v_r) + \frac{\rho v_r}{r} = S_m \dots\dots\dots (4)$$

Taking the time-average of scalar quantities and fluctuating velocity components, the continuity equations become as follow:

$$\frac{\partial \rho}{\partial t} + \frac{\partial}{\partial x_i}(\rho u_i) = 0 \dots\dots\dots (5)$$

While the momentum equation is transformed into the following time-average term:

$$\frac{\partial(\rho u_i)}{\partial t} + \frac{\partial(\rho u_i u_j)}{\partial x_j} = -\frac{\partial p}{\partial x_i} + \frac{\partial}{\partial x_j} \left[\mu \left(\frac{\partial u_i}{\partial x_j} + \frac{\partial u_j}{\partial x_i} - \frac{2}{3} \delta_{ij} \frac{\partial u_l}{\partial x_l} \right) \right] + \frac{\partial}{\partial x_j} (-\rho \overline{u'_i u'_j}) \dots\dots\dots (6)$$

Time averaging significantly reduce computational requirement of Navier-Stokes equation; however, it eliminate the prediction of another important phenomenon called turbulent flow. Turbulence is a random flow and highly time-dependent event which forms at high Reynolds number. To effectively use RANS equation; it needs to pair with a set of statistical models called turbulent models, specifically designed to handle turbulence.

Many approaches have been proposed by CFD practitioner to model turbulent flow, and some of it has become the main model to be used in CFD simulation software. In modelling high turbulent flow, two types of models are usually employed – k-epsilon and k-omega model. According to Best Practices for Turbulent Heat Transfer, these models possess the ability to handle complex flow and produce accurate results.

Listed below are the general forms of k-epsilon and k-omega turbulence model. The first model, k-epsilon, account for turbulent kinetic energy, k, and turbulent dissipation, ε, within the correlation. Given by the expression below,

$$\frac{Dk}{Dt} = \frac{\partial}{\partial x_k} \left[\left(\nu + \frac{\epsilon_m}{\sigma_k} \right) \frac{\partial k}{\partial x_k} \right] + \epsilon_m \left(\frac{\partial \bar{u}_i}{\partial x_j} + \frac{\partial \bar{u}_j}{\partial x_i} \right) \frac{\partial \bar{u}_i}{\partial x_j} - \epsilon \dots \dots \dots (7)$$

$$\frac{D\epsilon}{Dt} = \frac{\partial}{\partial x_k} \left[\left(\nu + \frac{\epsilon_m}{\sigma_\epsilon} \right) \frac{\partial \epsilon}{\partial x_k} \right] + c_{\epsilon 1} \frac{\epsilon}{k} \epsilon_m \left(\frac{\partial \bar{u}_i}{\partial x_j} + \frac{\partial \bar{u}_j}{\partial x_i} \right) \frac{\partial \bar{u}_i}{\partial x_j} - c_{\epsilon 2} \frac{\epsilon^2}{k} \dots \dots \dots (8)$$

While for k-omega, the model account for turbulent kinetic energy, k, and specific dissipation, ω. The model is as follow:

$$\frac{Dk}{Dt} = \frac{\partial}{\partial x_k} \left[\left(\nu + \frac{\epsilon_m}{\sigma_k} \right) \frac{\partial k}{\partial x_k} \right] + R_{ik} \left(\frac{\partial \bar{u}_i}{\partial x_k} \right) - \beta^* k \omega \dots \dots \dots (9)$$

$$\frac{D\omega}{Dt} = \frac{\partial}{\partial x_k} \left[\left(\nu + \frac{\epsilon_m}{\sigma_\omega} \right) \frac{\partial \omega}{\partial x_k} \right] + \alpha \frac{\omega}{k} R_{ik} \left(\frac{\partial \bar{u}_i}{\partial x_k} \right) - \beta \omega^2 \dots \dots \dots (10)$$

Where constants are given by, $R_{ik} = \epsilon_m \left(\frac{\partial \bar{u}_i}{\partial x_j} + \frac{\partial \bar{u}_j}{\partial x_i} \right)$,

Careful consideration needs to be taken when choosing the model to be used in simulating converging-diverging nozzle. Treatment on turbulence model analysis by Cebeci (2004) shown that k-omega is more effective when dealing with cases of flow near wall [15]. The case can be seen on the investigation of supersonic flow separation by Xiao et al (2007) which incorporate k-omega turbulence model into Reynolds Average Navier-Stokes (RANS) equation. Since converging-diverging nozzle geometry is small compared to total flow area, the flow can be assumed to be near nozzle wall. Thus, the usage of k-omega is most appropriate.

Many of the numerical models are embedded inside various commercial CFD softwares. The research study will focus more on the external factors which affect the accuracy of supersonic numerical solution. Factors studied are the use of appropriate algorithm, grid density, properties of material, to name a few.

CHAPTER 3:

METHODOLOGY

3.1 Grid Development

Experimental studies on mixing enhancement and supersonic flow separation by Papamouschou et al (2008) are used as main references. Information on the physical dimension of the geometry is extracted from the equipment used in the experiments. Shown below in Figure 3.1 is the schematic of the equipment used for the experiment on supersonic flow study in converging-diverging nozzle. From the equipment schematic, the information on converging-diverging part is then used as basis for development of computational domain.

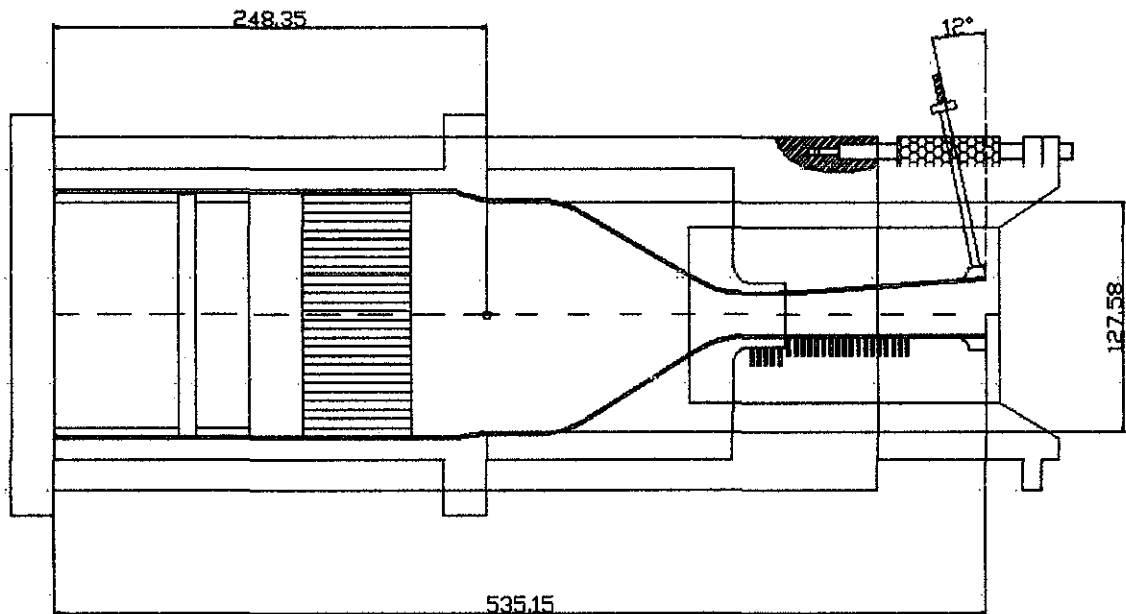


Figure 3.1: Nozzle setup used for experiment in Mixing Enhancement of Axial Flow and Supersonic Flow Separation in Planar Nozzle by Papamouschou et al (2008)

Papamouschou et al, in his work, has collected data on nozzles with different exit area to throat area ratios, A_e/A_t . In this paper, the study is primarily focus on one area ratio, which is $A_e/A_t=1.5$. The grid is developed using structured map scheme due to its simplicity and ability to cater for many cases. Under certain nozzle pressure ratio value, shock also known to extend outside the nozzle. Thus, the surrounding areas of nozzle outlet have been included as part of grid generated to observe the effect of nozzle exhaust stream. The surrounding area is denoted as pressure farfield. The diverging part is known to be more critical than the converging part, and in order to obtain more accurate result, grid with higher density is used at diverging section. Farfield is not a critical flow zone compared to diverging section of the nozzle and thus the grid density is made in lower density than the inner section of the nozzle.

Full scale size computational domain is shown in Figure 3.2(a). A focus view at converging-diverging section is shown in Figure 3.2(b). The grid is done based on the nozzle dimension stated in Papamouschou et al (2008), and several modifications have been made to suit the validation work. For example, instead of having full grid of nozzle and farfield, the validation work geometry is done only with half of the grid. This is done to reduce the computational expenses. However, several assumptions are made such that the flow is symmetry, which is the same for both top and bottom side of the nozzle and the flow is steady state.

As can be seen in Figure 3.2(a), the computational domain is divided into several zones – zone A, zone B, zone C, and zone D. Zone A is the top left farfield, zone B is the right farfield, and zone D is the bottom farfield located at the nozzle outlet. Among the farfield zones, zone D is the most important section since it shows the flow characteristics of exhaust stream. The last zone is zone C which represents the converging-diverging section.

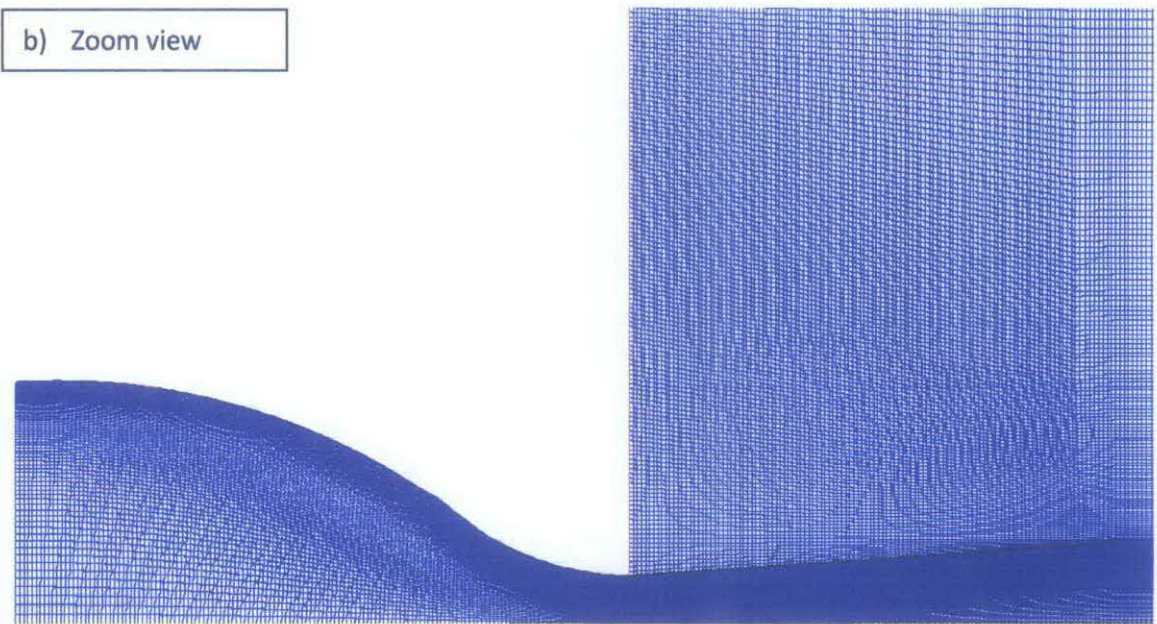
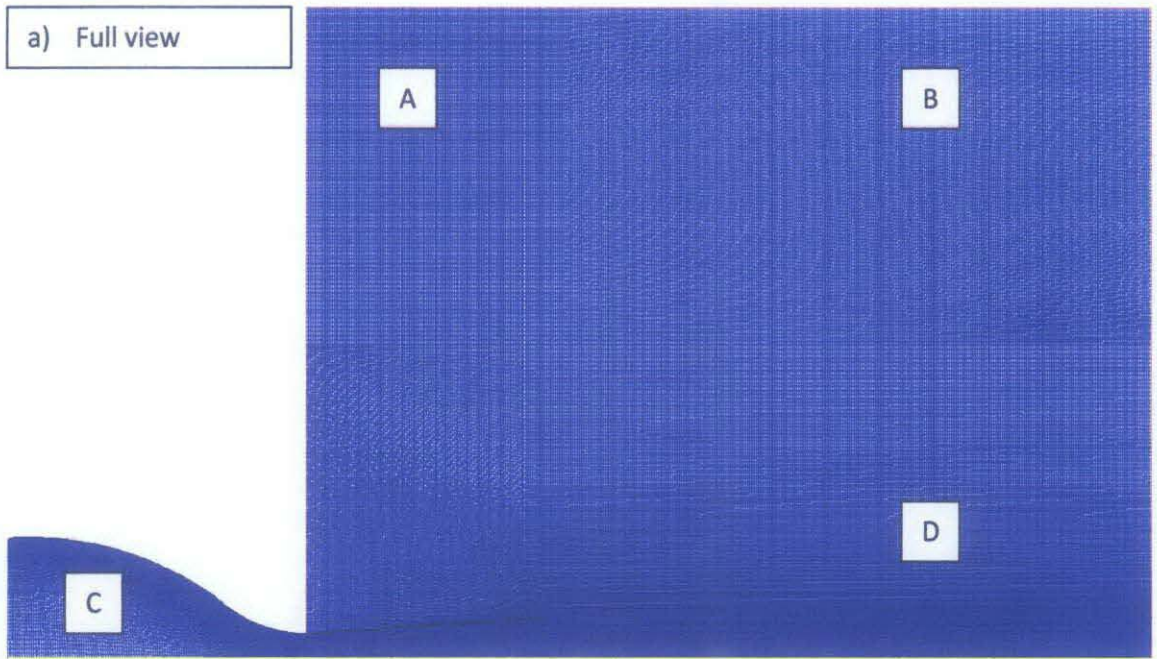


Figure 3.2: Computational domain for the simulation a) Full view, b) Zoom view into converging-diverging nozzle section

3.2 Simulation setup

The simulation is set up using numerical scheme that suit the compressible fluid system. Pressure-based solver is used while setting the computation to be 2D, axisymmetry. Since the system in study is a high speed compressible flow, highly turbulent flow is expected. Generally, Shock Capturing directly solves the Navier Stokes equation. Since directly solving the equations requires high computational power, it is simplified by averaging the fluctuating terms in Navier Stokes equation. The effect of turbulence is captured by adding a statistical model into the set of equations. Due to its ability to produce accurate approximation for near-wall flow [12], k-omega two-equation turbulence model is chosen. The solution error tolerance/residual is set to be 1E-6.

The simulation package utilize two-equation k-omega turbulent model in the following form:

Turbulent kinetic energy equation:

$$\frac{\partial(\rho k)}{\partial t} + \frac{\partial(\rho u_j k)}{\partial x_j} = P - \beta^* \rho \omega k + \frac{\partial}{\partial x_j} \left[\left(\mu + \sigma_k \frac{\rho k}{\omega} \right) \frac{\partial k}{\partial x_j} \right] \dots\dots\dots (11)$$

Dissipation rate equation:

$$\frac{\partial(\rho \omega)}{\partial t} + \frac{\partial(\rho u_j \omega)}{\partial x_j} = P - \beta \rho \omega^2 + \frac{\partial}{\partial x_j} \left[\left(\mu + \sigma_\omega \frac{\rho k}{\omega} \right) \frac{\partial \omega}{\partial x_j} \right] \dots\dots\dots (12)$$

As for simulation parameters, ambient conditions are set such that pressure is 14.85 psi, temperature is 290K, and freestream Mach number is 0.1 Ma. To investigate the effect of nozzle pressure ratio (NPR) on shock formation and flow pattern inside the nozzle, four NPRs are chosen which are NPR=1.27, NPR=1.34, NPR=1.47, and NPR=1.61, refer to Table 3.1.

Table 3.1: List of nozzle pressure ratio used for investigation

| Case | NPR (Po/Pamb) | Stagnation Pressure, Po (Pascal) |
|------|---------------|----------------------------------|
| 1 | 1.27 | 130031.6754 |
| 2 | 1.34 | 137198.7756 |
| 3 | 1.47 | 150509.1046 |
| 4 | 1.61 | 164843.3051 |

The result from the simulation is then compared with image obtained from experimental studies, as shown in Figure 3.3 as well as pressure distribution data from the nozzle flow, as shown in Figure 3.4.

Figure 3.3 will be used to compare the exhaust/plume at the outlet of the nozzle, primarily to examine the closeness of flow pattern predicted by computational model. The plume, generated by flow separation phenomena, is the main mechanism of mixing enhancement. Thus, it is very important to note how much the simulation can produce similar flow pattern.

In Figure 3.4, there are two parameters significant for comparison. The first one is the shock location, and the second one is the shock pressure pressure at which shock start to form. Looking at the experimental data, it shows a trend. As nozzle pressure ratio (NPR) increase, the shock location increase and the pressure at which shock starts to build decrease. It is significant to note not only the value of the shock location and shock pressure but the trend as well. Examinations of values enable to relate the data to the accuracy of computation, while trend will reveal the precision or closeness of the computation data to the experimental data.

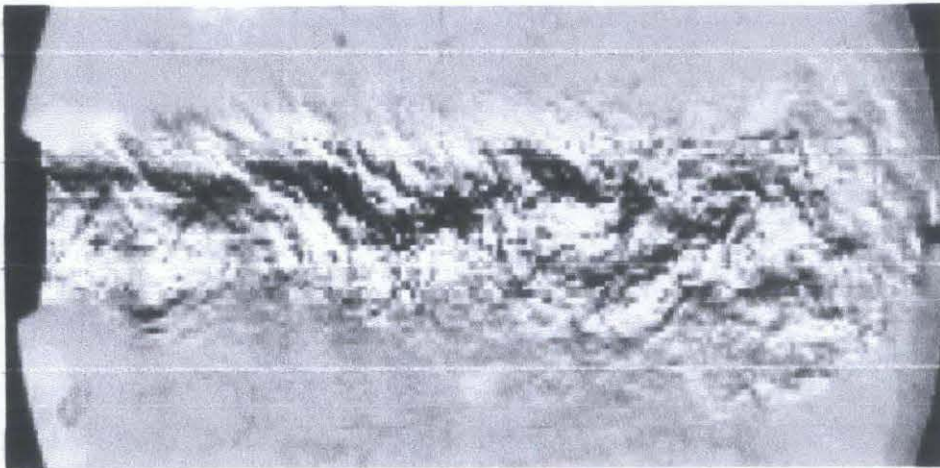


Figure 3.3: Schlieren image of nozzle plume. Taken from Mixing Enhancement studies by Papamouschou (2000)

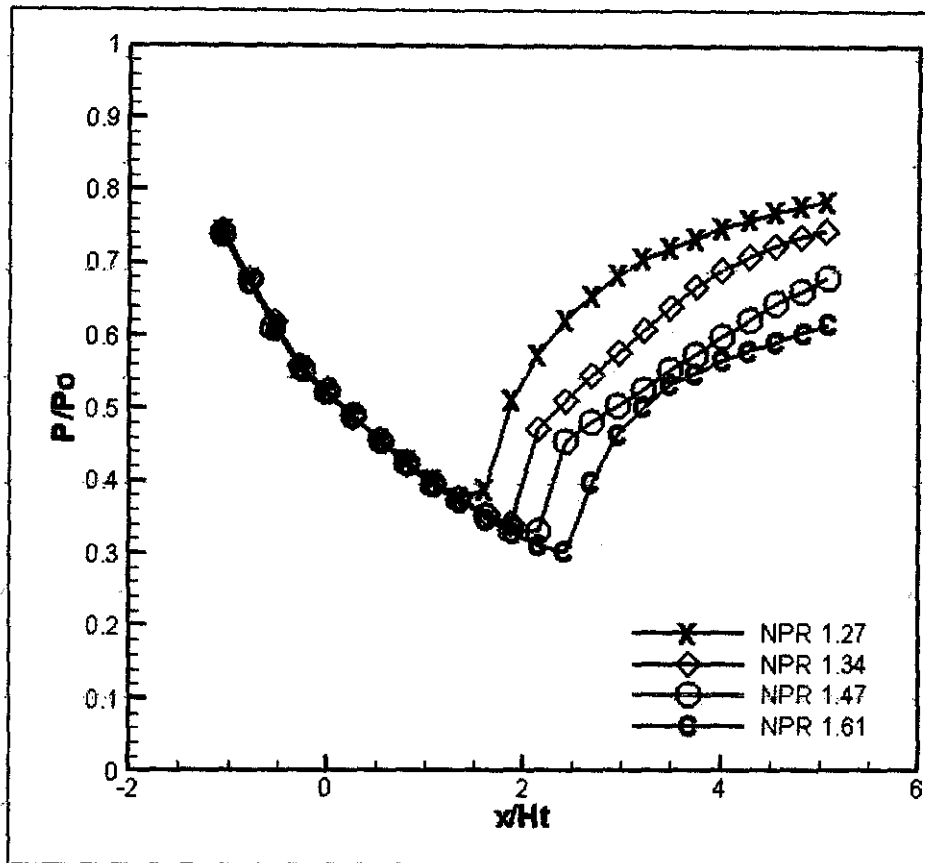


Figure 3.4: Experimental data of pressure distribution at nozzle topwall, taken from supersonic flow separation studies by Papamouschou et al (2008)

Table 3.2: Experimental shock pressures and shock locations under different NPRs

| NPR | Shock pressure (Approx) | Shock location (Approx) |
|------|-------------------------|-------------------------|
| | Trend: Decreasing | Trend: Increasing |
| 1.27 | 0.4 | 1.5 |
| 1.34 | 0.35 | 1.7 |
| 1.47 | 0.33 | 2 |
| 1.61 | 0.3 | 2.3 |

3.3 Grid Refinement Study

Accuracy of a result is influenced by many factors – one of it is grid size. Generally, the higher the grid density, more accurate result can be achieved (even though that is not always the case). In contrast, higher density mesh contains more nodes and solving sets of partial differential equations will requires more computational power. Refinement of grid is infinite, it can be done many times, but the solution residual level is not.

There is a point whereby refining the grid further will not improve the accuracy of the solution – this is the grid independency point and it provides the optimum grid size. Computation using further refine meshes is only a waste of processing power since the solutions produced are almost on the same accuracy level as the optimum size mesh.

To identify the optimum grid size, a grid dependency test study is conducted using refined meshes with different density. The gas flow in axial direction while velocity profile and shocks forms radially in the nozzle. Refinement direction is suspected to present significant impact to the solution accuracy. The effect of direction of refinement will be studied. Thus, the meshes are refined in three different directions which are axial direction, radial direction, and both axial radial direction.

Table 3.3 List of meshes with cell and face size

| Mesh | Cell Size | Face Size |
|---------------|------------------|------------------|
| Original Mesh | 137990 | 276963 |
| Axial 1 | 171855 | 344958 |
| Axial 2 | 368680 | 739443 |
| Radial 1 | 146300 | 293598 |
| Radial 2 | 201700 | 404498 |
| Axi Radi 1 | 182925 | 367113 |
| Axi Radi 2 | 426500 | 854831 |

Starting with the original mesh, for each direction, the refinement is made twice. The second refinement mesh has higher grid density than the first. There are a total of seven meshes developed for grid refinement study, listed in Table 3.3 together with the cell size and face size. Higher cell and face size indicates higher value of density.

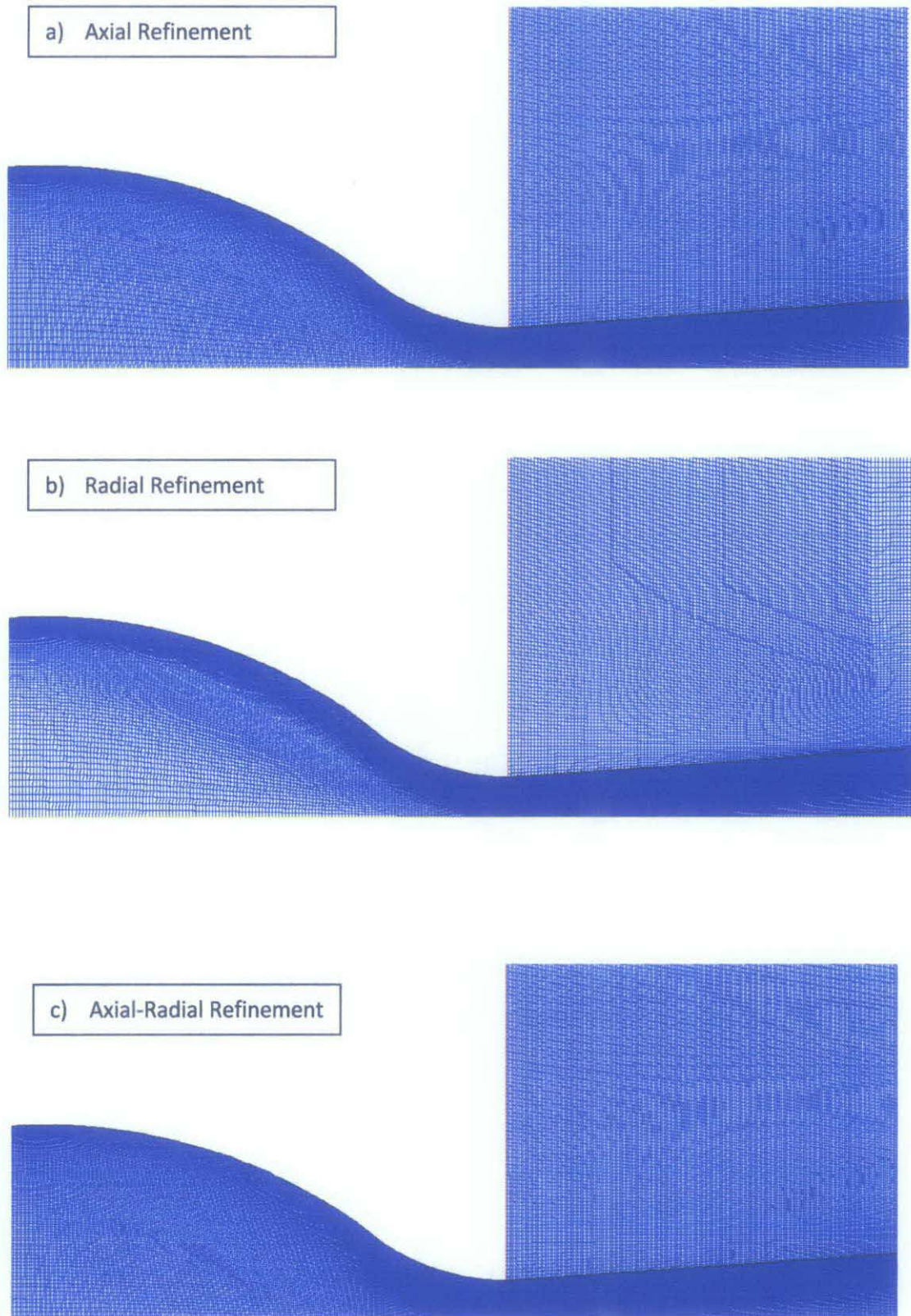


Figure 3.5: Mesh after refinement in three different directions, a) Axial, b) Radial, c) Axial - Radial

3.4 Data Visualisation

After the solution reaches a certain residual level, the data will need to be converted into a presentable form. Data is extracted from region of interest - pressure change at the centreline as well as at the topwall of nozzle. Since we are interested at the change in pressure along the nozzle, a plot of pressure versus nozzle length is suitable. It is easy to notify the presence of shock by observing the condition of the pressure at the diverging section. Gradual reduction followed by sudden jump in pressure is an indication of shock.

Another effective means of detecting shocks is by using contour. The use of contour will enable the user to observe the gradient of flow parameter in the fluid region. Shock will be at the position where a region concentrated with flow field followed by a region with low concentration of flow field. The boundary between the high concentration and low concentration of flow field is the shock layer. The results of the simulation will be discussed in the Section 4: Result and Discussion using the two proposed visualisation method.

CHAPTER 4:

RESULT AND DISCUSSION

In analysing gas flow in converging-diverging nozzle, two sections are observed. First, part with the highest degree of shear stress – the wall; and second, the part that is least affected by shear stress – the nozzle centreline. Analysing pressure distribution in the nozzle section as can be seen at Figure 4.1, the fluid experience expansion, compression, and then recovery [3].

The trend shows that gas expansion start from the converging section of the nozzle up till before shock takes place, depending on NPR values. Compression on the other hand always occurs at the diverging section of the throat, and it is where formation of shocks occurs. Different NPR values will produce different magnitude of exit pressure, and thus affect the location of shock. Lastly, recovery phase is also observed where the gas slowly recovering its pressure until it reaches nozzle exit. Ideally the gas will recover its original pressure. However, in reality, a portion of energy is converted into heat (energy loss to environment) during compression process and it is an irreversible process [4]. Therefore, the gas will not be able to recover the initial pressure.

Evaluating the computation result at nozzle centreline, the location is close to the nozzle throat ($x=0$). Flow at different NPR also experience shock at different pressure value. As seen in Figure 4.1, the shock forms closer to the nozzle throat with smaller NPRs. The evolution of shock is highly affected by nozzle operating pressure – nozzle at smaller NPR will experience large downstream pressure in comparison to pressure at shock location. The magnitude of back pressure is high enough to be able to push the shock upstream and prevent it from moving further downstream of the nozzle.

The information on shock at the wall of the nozzle shows similar trend as in nozzle centreline but with different flow behaviour. Referring to Figure 4.3, the pressure distribution is almost similar to those of centreline especially at the recovery phase. However, during expansion phase, the pressure distribution is not as smooth as in centreline. One of the causes is the interaction of boundary layer with shock wave, which is known to induce instabilities to the flow regime.

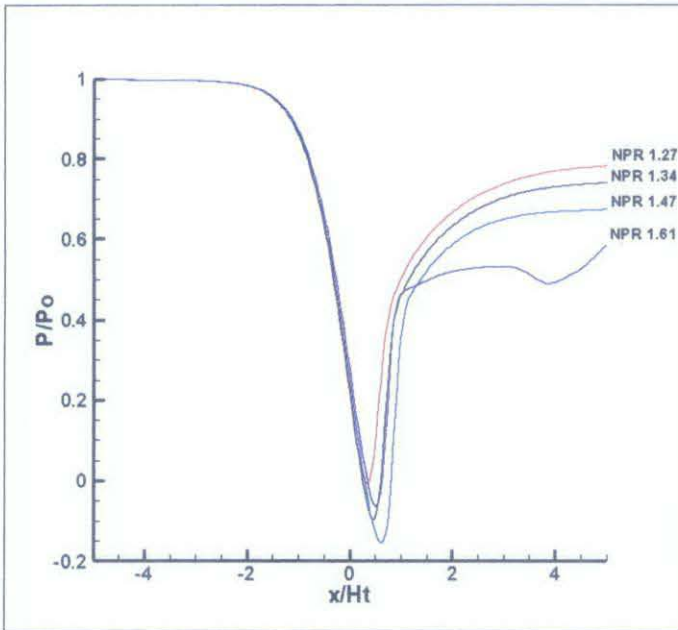


Figure 4.1 Centreline pressure distributions of original mesh

4.1 Grid Refinement Analysis

Looking at the computational result, it can be seen that the jump is not sudden. It takes several grids for the compression to occur before recovery took place. A shock is defined as an instantaneous jump in fluid properties, and thus the pressure should not take many grids to elevate. This phenomenon is called solution smearing which is caused by round-off errors. Barter and Darmofal (2010) stated that artificial viscosity is usually the main factor which causes solution smearing over several grids.

Many factors might contribute to the inaccuracy of the solution. Apart from computational algorithm, the grid size of a model also affects the accuracy. Mesh refinement study is usually investigated by studying the effect of size only. However, in this case, refinement direction is also taken into account. Refinement is made to the mesh in three different directions – a) axial, b) radial, and c) both axial and radial direction.

Pressure distribution across nozzle at centreline and topwall are analysed and compared to evaluate the effect of mesh refinement. By analysing two factors – grid density and refinement direction, it is expected to discover the optimum density as well as most effective refinement direction.

4.1.1 Effect of Grid Density

In each direction, two mesh sizes are chosen for display. Mesh 2 is of higher density than Mesh 1. Among the three types of meshes, mesh refined at both axial and radial direction has the highest density. The results obtained from mesh of different refinement direction are compared by analysing the pressure distribution at nozzle centreline. Analysis is made using the pressure distributions data of NPR1.27 from all the abovementioned meshes.

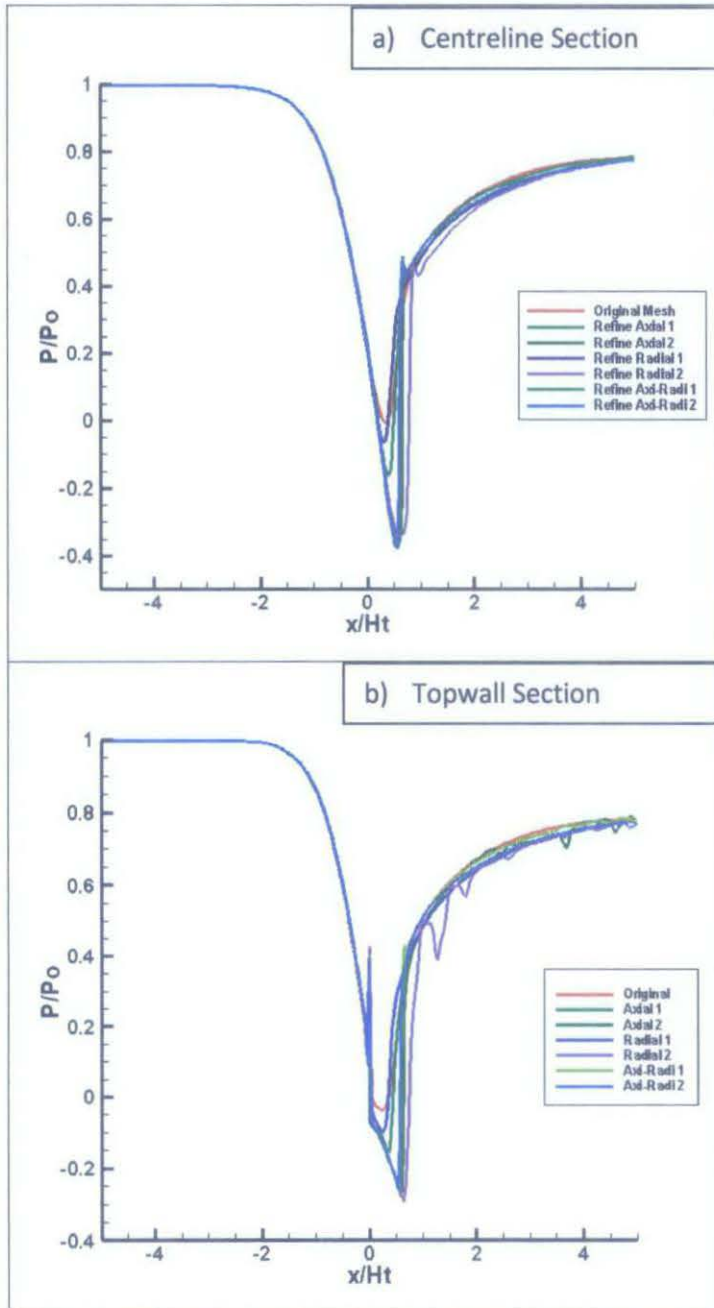


Figure 4.2: NPR 1.27 pressure distributions on different grid refinement direction at a) Centreline Section, b) Topwall Section

From Figure 4.2, it is observed that as the density of cells increases, the computation shows larger expansion before the shocks. The use of higher density meshes also result in considerable reduction of degree of smearing as the pressure jump is more rapid compared with lower density meshes. Availability of larger number of nodes in high density mesh has enable computation with lesser round-off error and increase in degree of accuracy. The phenomena is similar in both centreline and topwall pressure distribution.

Apart from that, meshes with higher density (Axial 2, Radial 2, Axial-Radial 1, and Axial Radial 2) also enable prediction of weak shocks, which are observed as a small fluctuation (or jump) after the main shock. Weak shocks are observed by Papamouschou et al (2008) in his experiments. No sign of weak shock visible in the computation using lower density meshes.

It is well known that fluid will form a boundary layer at the place with high shear stress, which in this case, the wall. Interaction of shock with boundary layer has contributed to pressure loss and increase in turbulent level at the wall, creating unsteadiness and instabilities in the flow pattern [16]. Looking into Figure 4.2(b), instability is observed in topwall pressure distribution. The instabilities are visible for computation using Axial 2 and Radial 2 meshes. Pressure fluctuation is not visible on the result with lower density meshes. Thus, it indicates that by using mesh with higher density, more accurate capture of shock pattern (weak shocks and shock-boundary layer interaction) is obtained.

The plot also shows four meshes with almost similar results which are Refine Axial 2, Refine Radial 2, Refine Axi-Radi 1, and Refine Axi-Radi 2. It is a sign of grid independency because even by using Refine Axi-Radi 2, which is shown from Table 3.3 as having the largest cell size, the result does not have significant improvement with the other two meshes. From Table 3.3, among the four meshes, Refine Axi-Radi 1 is the smallest in cell size which is 182935. Using the data above, the mesh with optimum size is Refine Axi-Radi 1 and it will be used for further computation.

4.1.2 Effect of Grid Refinement Direction

As stated previously, the grid refinement study will focus on two factors which are grid density and grid refinement direction. In this section, comparison of mesh is made against different refinement directions. The result is then compared with experimental data, refer to Figure 3.3.

4.1.2.1 Axial Refinement

Based on Figure 4.3(a) and Figure 4.3(b), it is observed that refinement at axial direction improved the computational result in terms of discontinuity approximation. The compression still takes several grids to develop but it is more rapid. Discontinuity is better approximated in axial direction because of higher number of nodes at the direction of flow.

However, the shock location is affected – it no longer follows the previous discussion at which the shock location is moving to downstream with higher NPRs. The computation predicts formation of shocks at almost the same location, and it is very close to the nozzle throat. Higher operating pressure is known to produce shocks further downstream due to lower exit pressure. Since the location is not following the experimental data, the predicted shock location information from axial refinement mesh is not reliable.

Apart from that, only NPR 1.27 and NPR 1.34 shows significant improvement in shock representation but in exchange, the degree of gas expansion is predicted larger. Based on experimental result, the predicted shock location is not accurate. The other two NPRs – NPR 1.47 and NPR 1.61 does not show evident of improvement in terms of rapidity of compression. The result shows high degree of inaccuracy and over-prediction, and thus, is not acceptable.

4.1.2.2 Radial Refinement

Figure 4.3(c) and Figure 4.3(d) which shows the result of radial refinement provides sign of improvement on discontinuity approximations. The compression is rapid for all NPRs and quickly follows by pressure recovery. Even though the discontinuity is not as rapid as those predicted with axially refined meshes, it shows that radial refinement is able to provide improvement in terms of discontinuity.

In addition, location of shock agrees with trend in experimental result which shows shock location forms at further downstream with larger NPR. Even though the computational result follows the trends, in term of accuracy, the result is showing error. Shock location of NPR 1.27 predicted by computation is at the location of 0.3 units while from experimental data, it is suppose to be approximately at 1.5 units from the throat. Similar deviation happens to other NPRs as well.

Another deviation founds is the prediction of pressure ratio at which shock starts to develop. Shock is predicted to form at pressure ratio lower than shown by experimental data. The computation shows shock develops at negative pressure value, which means lower than ambient pressure. Based on experimental data, the shock pressure should not be less than ambient, and it is suppose to be at the range of 0.4 for NPR 1.27 to 0.3 for NPR 1.61.

Therefore, it is found that radial refinement provide significant improvement in terms of precision (following the trends) of both shock location and shock pressure but significantly lacking in terms of accuracy (closeness to real values).

4.1.2.1 Axial-Radial Refinement

As for Figure 4.3(e) and Figure 4.3(f), refinement on both axial and radial direction seems to produce larger degree of smearing over the grids. Compression process, which supposes to be instantaneous, is predicted to forms over larger grid area inside the divergent section. Computed shock location also behaves similarly to axial refinement – the shocks form around the same location close to nozzle throat.

Numerical inaccuracy of pressure during compression phase happens to all NPRs value. However, the result is most satisfactory in terms of predicting the pressure ratio value during formation of shocks. For all NPRs, the shock pressure is computed to be higher than ambient, which is correct. In terms of accuracy, the computed shock pressure is slightly deviating from experimental data. Shock pressure at NPR 1.27 and 1.61 is under-predicted at pressure ratio of 0.34 units and 0.12 units– with a deviation of only 0.06 units and 0.18 units respectively.

Therefore, qualitatively, it is found that mesh refinement at both axial and radial direction gives better approximation in following the trends of shock pressure, but did not provide satisfactory result in following the trend of shock location in

experimental data. In terms of accuracy, refinement in both axial and radial direction provides the best result, with only slight deviation from experimental data.

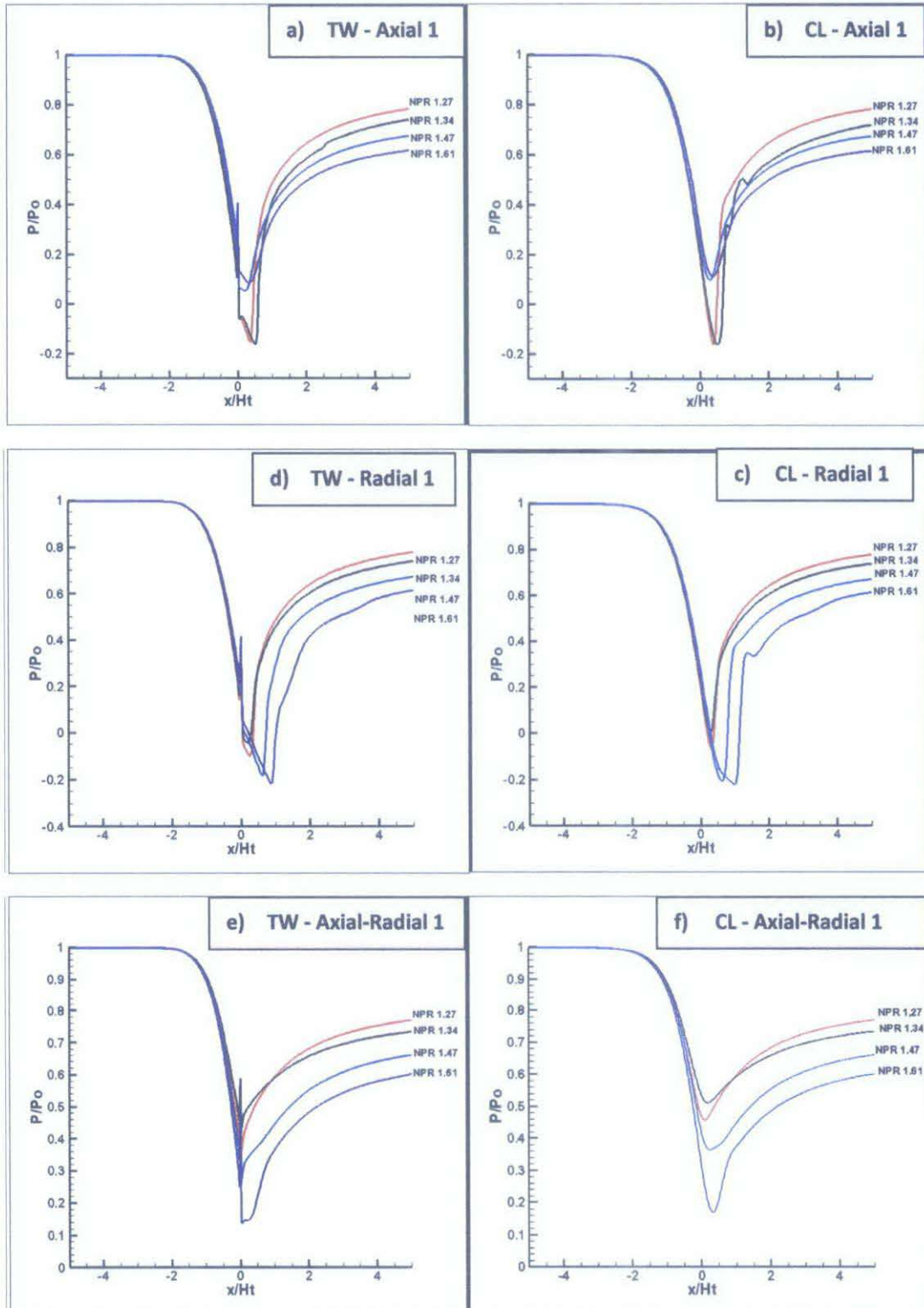


Figure 4.3: Nozzle pressure distributions at nozzle centerline (CL) and topwall (TW) using axial 1, radial 1, and axi-radi 1 mesh

Table 4.1: Predicted shock pressure and shock location of nozzle topwall, and deviation from experimental values

| a) Refine Axial 1 | | | | |
|---------------------------------|-----------------------|------------------|-----------------------|------------------|
| NPR | Shock Pressure | Deviation | Shock Location | Deviation |
| 1.27 | -0.15 | 0.55 | 0.4 | 1.1 |
| 1.34 | -0.15 | 0.5 | 0.5 | 1.2 |
| 1.47 | 0.05 | 0.28 | 0.2 | 1.8 |
| 1.61 | 0.1 | 0.2 | 0.4 | 1.9 |
| Average | | 0.3825 | | 1.5 |
| b) Refine Radial 1 | | | | |
| NPR | Shock Pressure | Deviation | Shock Location | Deviation |
| 1.27 | -0.1 | 0.5 | 0.3 | 1.2 |
| 1.34 | -0.05 | 0.4 | 0.3 | 1.4 |
| 1.47 | -0.2 | 0.53 | 0.5 | 1.5 |
| 1.61 | -0.25 | 0.55 | 0.9 | 1.4 |
| Average | | 0.495 | | 1.375 |
| c) Refine Axial-Radial 1 | | | | |
| NPR | Shock Pressure | Deviation | Shock Location | Deviation |
| 1.27 | 0.34 | 0.06 | 0 | 1.5 |
| 1.34 | 0.4 | -0.05 | 0 | 1.7 |
| 1.47 | 0.26 | 0.07 | 0 | 2 |
| 1.61 | 0.12 | 0.18 | 0 | 2.3 |
| Average | | 0.065 | | 1.875 |

Displaying the discussion above in numerical forms will assist in analysing the degree of deviation for each refinement scheme. Table 4.1 shows the predicted values together with deviation from experimental data. The average deviation for each refinement scheme is calculated to observe overall deviation trend. As suspected, refinement in both axial and radial direction provides the least error in predicting shock pressure with only average deviation of 0.065. This shows that the predicted shock pressure is very close to experimental data. Refinement in radial direction also proved to be the best scheme in predicting shock location with average deviation of 1.375. The result indicates that the predicted shock location is largely deviating from experimental data but still follow the trend.

Despite that, axial-radial refinement is shown to present largest error during prediction of shock location, with an average deviation of 1.875, and refinement in radial direction is producing largest average deviation of 0.495 in prediction of shock pressure. Axial refinement is showing average performance in predicting both shock location and pressure. The result successfully proves that refinement direction is affecting numerical performance of a simulation. Thus, careful selection of mesh refinement scheme is needed to obtain mesh which can provide optimum computational performance and accuracy.

4.1.3 Small and large NPRs computational result comparison

To evaluate the effect of refinement in topwall and centreline pressure distribution more closely, two NPRs are chosen, which is NPR1.27 and NPR 1.61. Extracted from the same computational data as Figure 4.2, the difference in computational accuracy is clearer. Observing Figure 4.4(a), it is clear that gas expansion has been predicted larger than it suppose to be. Experimentally, shock at NPR1.27 should form at higher value for smaller NPR. However, computational result produces different shock pressure. Shock location is also on the same spot for both NPRs which are not accurate.

Different from axial refinement, radial refinement produces a result that agrees with trend of experimental data. Location of shock agrees with experimental data – smaller NPR will produce shock closer to the throat. Satisfactory discontinuity

approximation is observed and pressure jump is rapid. The pressure ratio at which shock forms is larger at smaller NPR. However, looking at the trend is not enough because when analysing the value of pressure predicted, it seems to be very small compared to experimental result. Thus, radial refinement produces result with desirable trend on both shock location and shock pressure but not accurate.

Looking at Figure 4.4(c), refinement at both axial and radial direction produces result that shows shock location close to nozzle throat for both NPRs. This is not aligned with experimental result. Discontinuity also has been poorly approximated and as a result, the jump is no longer rapid but smearing larger than axial refinement scheme. Trend of pressure ratio of shock formation has been predicted quite satisfactorily by this refinement scheme.

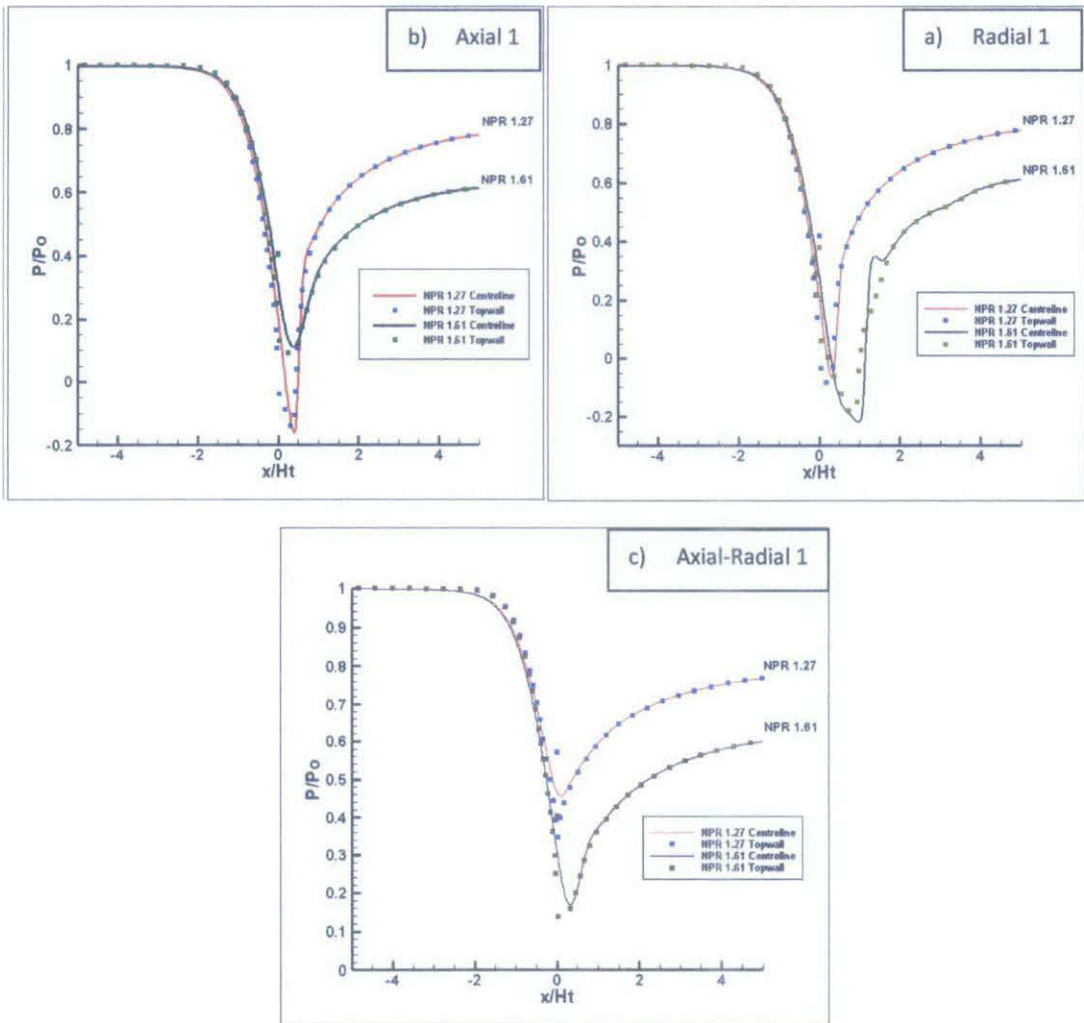


Figure 4.4: Comparison of pressure distribution between small and large NPR values. Refinement direction a) Axial, b) Radial, c) Axial-Radial

4.2 Shock Structure Evaluation

The formation is clear when evaluating the pressure distribution across nozzle but it did not give a clear view on the flow characteristics. Contour is the best tool to evaluate the flow pattern by looking at the parameter gradients. Parameter chosen to evaluate is velocity magnitude. Interaction between fluid structures will affect properties of fluid as well as flow parameters, including the velocity of fluid. Thus, evaluation of velocity magnitude will enable view on flow pattern. In this section, to allow more accurate observation on flow pattern, data obtained from Refine Axial 2, Refine Radial 2, and Refine Axi-Radi 2 meshes are used.

From Figure 4.5, shock is located at the point of highest velocity magnitude. Velocity gradient shows that the fluid velocity gradually increasing at the point approaching nozzle throat. Once the fluid reaches the throat, the velocity magnitude rapidly increases and reaches supersonic – indicated by red colour. After that the gradient is seen to slowly decreasing to low velocity magnitude. An interesting phenomenon occurs at nozzle outlet stream – the exhaust stream shows sign of instable plume which is also observed by Papamouschou and his team.

Closer inspection on the contour provide evident that the instability has started after the shock. Clear view of the instability can be seen at Figure 4.6(a). According to Simpson and White (2005) and Papamouschou (2008), this is the effect of interaction between shock and boundary layer. Instability cause by shock-boundary layer interaction will also produce undesirable oscillation in the nozzle [5]. If not controlled, the oscillation will achieve resonance and will reduce the life span of equipments. Comparing between the three flow-patterns in Figure 4.5(a), 4.5(b), and 4.5(c), each mesh capture different kind of plume pattern; the pattern in the nozzle is almost similar.

Comparing the plume pattern of simulation data from those of experimental data, the simulation result Axial 2 mostly resembles the exhaust plume shown in Figure 3.3. Result from Radial 2 and Axial-Radial 2 shows significant difference from image obtained from experiment. To explain this situation, we can refer back to Table 4.1. Average numerical performance without severe deviation by axial refinement in both shock location and shock pressure has enables it to provide the best overall picture of flow pattern among the three.

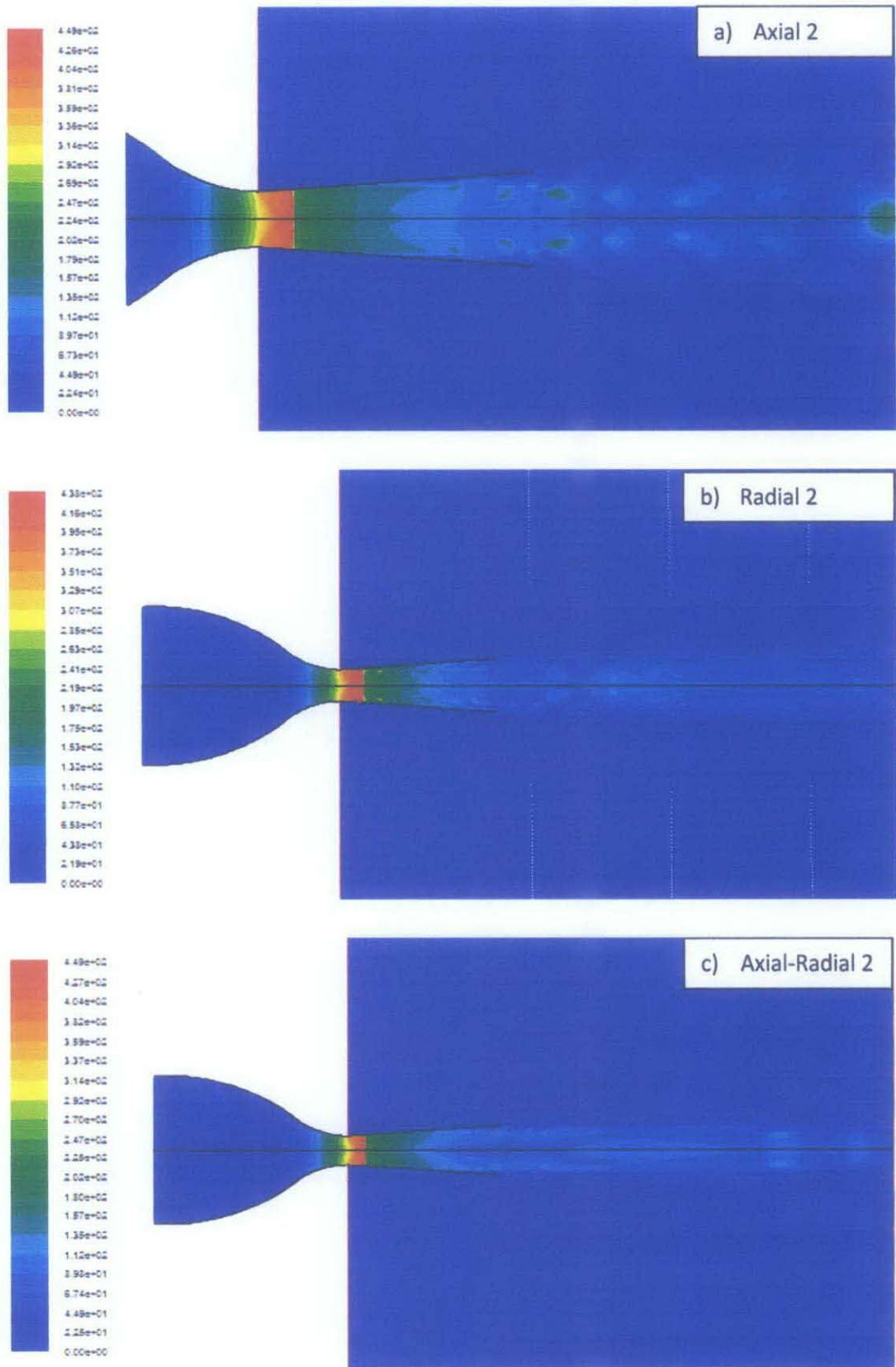


Figure 4.5: Flow pattern of NPR 1.27 condition inside the nozzle from three different meshes a) Axial 2, b) Radial 2, c) Axial-Radial 2

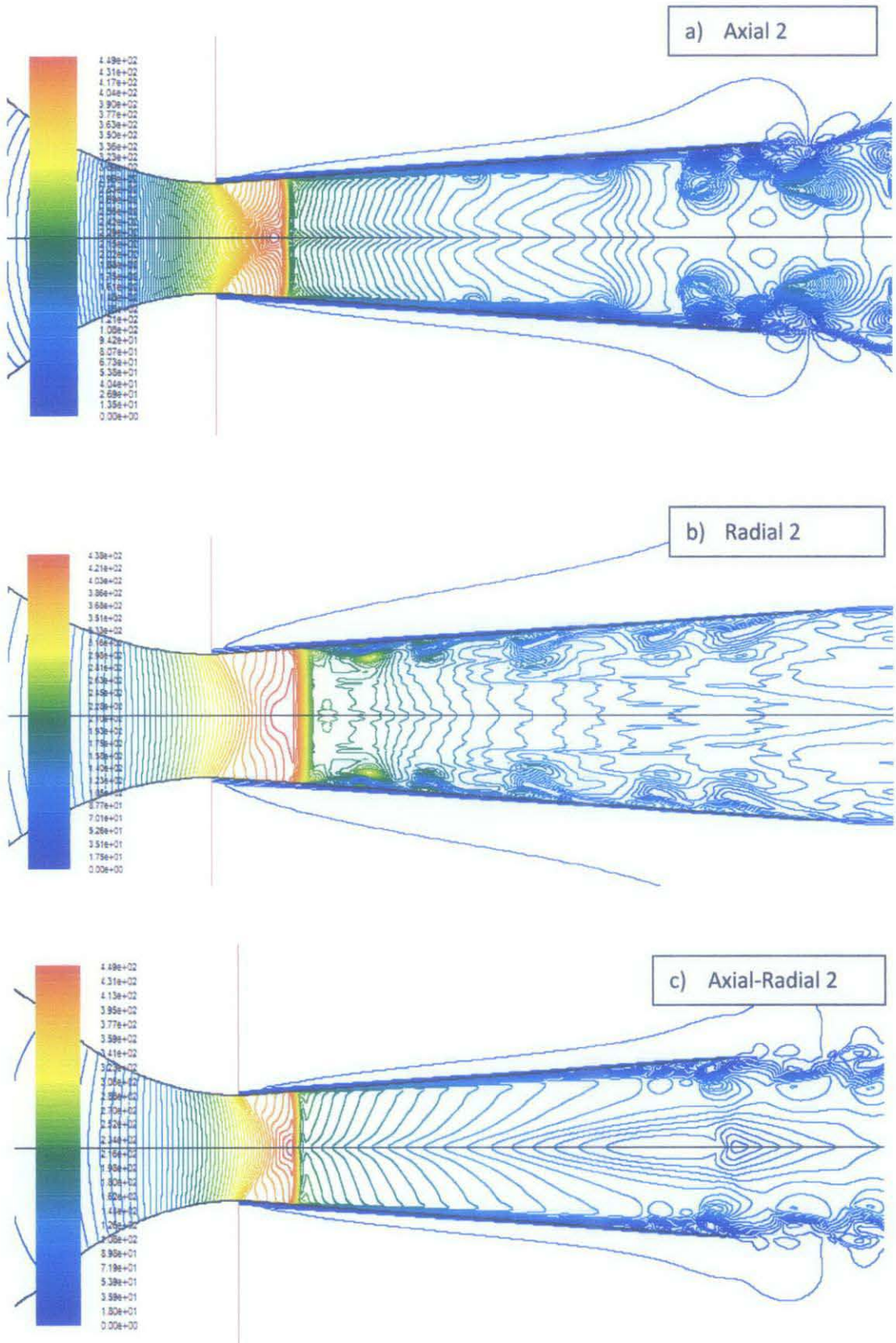


Figure 4.6: Contour of velocity magnitude a) Axial 2, b) Radial 2, c) Axi-Radi 2

To get clearer view on the shock shape, level of velocity gradients in contour plot is reduced. Looking at velocity contour of NPR 1.27 for Axial 2, Radial 2, and Axial-Radial 2 meshes, clearly the shock sits near the nozzle throat. Under the simulation parameter, the shock takes a shape of a normal shock – a type of shock that looks like a vertical straight line [4]. It shows that all meshes are able to capture the shape of shock accurately.

Apart from that, Figure 4.6 also shows presence of separation bubbles right after the nozzle. The bubbles are still small at NPR 1.27 and but it already contain enough energy to cause the flow to separate from the wall. Shock-boundary layer interaction is seems to cause unstable flow and loss of pressure. Further examination and analysis into Figure 3.3, it is found that the instability causes mixing enhancement effect to take place at the nozzle exhaust following the experiment by Papamouschou et al (2000).

CHAPTER 5:

CONCLUSION AND RECOMMENDATION

5.1 Conclusion

The simulation shows that under different nozzle operating pressure, formation of shocks will be largely affected in terms of shock location and shock strength. Under these investigated NPRs, normal shock with varying shock pressure is produced. At higher NPRs, the final pressure after recovery is found to be lower than those of low NPRs. Therefore, location of shocks is found to be further downstream with higher operating pressure due to lower magnitude of back-pressure.

Different behaviour of flow pattern is also observed at the nozzle wall and nozzle centreline. At centreline, clean pressure distribution is obtained indicating smooth flow on that area. On the other hand, flow pattern at nozzle topwall shows significant unsteadiness and pressure fluctuation. Pockets of separation bubble and increase in turbulent level are observed which primarily caused by shock-boundary layer interaction.

Further study on mesh refinement confirms that refinement scheme is indeed a factor affecting computational accuracy. From the result discuss about effect of grid density, it can be concluded that the optimum size mesh to be used in the simulation is Refine Axial-Radial 1 mesh. As for refinement direction, refinement in radial direction gives the best accuracy in following the shock location trend of experimental result. Using this refinement scheme, prediction on shock location follows closely to the expected trend. But since the deviation is quite large, it is lacking in terms of accuracy of the solution.

Refinement in both axial and radial on the other hand, produces result which does not follow the experimental shock location trend. But when looking into the result especially on shock pressure, satisfactory degree of accuracy is obtained. Deviation of predicted shock pressure from experimental data is very small.

Lastly, refinement in axial direction shows average prediction performance in terms of shock location as well as shock pressure. Due to its average performance, axial refinement does not exhibit severe deviation and thus is able to provide better

evaluation of nozzle flow pattern. Meaning that refinement in axial might not help to improve the accuracy of the computation, but it will help in terms of visualisation of the flow.

It is also found that higher density meshes have the capability to improve Shock Capture solution in terms of predicting accurate flow pattern such as weak shocks and instabilities caused by shock-boundary layer interaction. Weak shock is trivial compare to main shock, and lower mesh is found to be not capable of capturing trivial flow pattern.

Thus, based on the discussion above, it can be concluded that refinement in radial direction will improved the ability of the computation to follow closely the expected trend of shock location, but sacrificing the accuracy of the solution. While refinement in both axial and radial direction helps to improve accuracy of solution and follow the trends for shock pressure, but did not improve the capability to follow expected trends in shock location.

5.2 Recommendation

During the study, it is found that shock location, shock strength, as well as shock pattern predicted by numerical computation is deviating from the experimental data. Most of the time, the problem is due to the lack of accurate model to be used as turbulent model as well as discretization model.

For future study, improvement on Shock Capturing scheme need to be done as the current models is not able to improve mathematical performance of Shock Capture in order to produce accurate result, mostly the point of discontinuity. Flow patterns are also not accurately captured, especially at the part where weak shocks suppose to be present.

Without accurate discontinuity approximation model, the computation will not be able to accurately capture flow pattern after the shocks as well as shocks location.

Further analysis need to be done to analyse the effect of mesh refinement to computational accuracy. After this, the effect of mesh interval size should be studied. The result should reveal the best combination of interval sizes within the mesh.

CHAPTER 6.0

REFERENCE

- [1] S. T. Geoffrey Brooks, Peter Witt, M.N.H. Khan, and Michael Nagle, "The Carbothermic Route to Magnesium," *Journal of Metallurgy*, 2006.
- [2] D. Papamoschou, "Mixing Enhancement using Axial Flow," in *38th Aerospace Sciences Meeting and Exhibit*, Reston, VA, 2000.
- [3] Q. Xiao, *et al.*, "Numerical investigation of supersonic nozzle flow separation," *AIAA Journal*, vol. 45, pp. 532-541, 2007.
- [4] J. D. Anderson, "Modern Compressible Fluid, with Historical Perspective," 2004.
- [5] P. Ott, *et al.*, "Experimental and numerical study of the time-dependent pressure response of a shock wave oscillating in a nozzle," *Journal of Turbomachinery*, vol. 117, pp. 106-114, 1995.
- [6] D. Papamoschou, "Mixing Enhancement Using Axial Flow," *AIAA Journal*, 2000.
- [7] D. Papamoschou, *et al.*, "Supersonic nozzle flow separation in Planar Nozzles," *Journal of Shock Waves*, 2008.
- [8] G. Brooks, *et al.*, "The carbothermic route to magnesium," *JOM*, vol. 58, pp. 51-55, 2006.
- [9] D. A. Simpson and A. J. White, "Viscous and unsteady flow calculations of condensing steam in nozzles," *International Journal of Heat and Fluid Flow*, vol. 26, pp. 71-79, 2005.
- [10] R.S.M. Chue, *et al.*, "Design of a shock-free expansion tunnel nozzle in HYPULSE," *Journal of Shock Waves*, vol. 13, pp. 261-270, 2003.
- [11] A. Bonfiglioli and R. Paciorri, "Comparative study of stagnation point anomalies by means of shock capturing and shock fitting unstructured codes," in *6th European Symposium Aerothermodynamics for Space Vehicles, November 3, 2008 - November 6, 2008*, Versailles, France, 2009.
- [12] J. D. Anderson, "Computational Fluid Dynamics, The Basics and Application," 1995.
- [13] G. E. Barter and D. L. Darmofal, "Shock capturing with PDE-based artificial viscosity for DGFEM: Part I. Formulation," *Journal of Computational Physics*, vol. 229, pp. 1810-1827, 2010.
- [14] S. Gottlieb, *et al.*, "Recovering high-order accuracy in WENO computations of steady-state hyperbolic systems," *Journal of Scientific Computing*, vol. 28, pp. 307-318, 2006.
- [15] T. Cebeci, *Analysis of Turbulent Flows*, 2nd Edition ed.: Elsevier.
- [16] K. Sinha, *et al.*, "Modeling the Effect of Shock Unsteadiness in Shock-turbulence boundary layer interaction," 2005.

7.0 APPENDIX 1: Gantt Chart of FYP1 Activities

7.1 Gantt Chart of FYP I

| Num | FYP1 Activities | 1 | 2 | 3 | 4 | 5 | 6 | 7 | 8 | 9 | 10 | 11 | 12 | 13 | 14 |
|-----|----------------------------------|---|---|---|---|---|---|---|---|---|----|----|----|----|----|
| 1 | Selection of Project Topic | █ | █ | | | | | | | | | | | | |
| 2 | Literature Review | | █ | █ | █ | █ | █ | █ | █ | | | | | | |
| 3 | Submission of Preliminary Report | | | | | █ | | | | | | | | | |
| 4 | Seminar 1 | | | | | █ | | | | | | | | | |
| 5 | Validation Activities | | | | | | | | | | | | | | |
| | Analyzing cases for validation | | | | █ | █ | █ | █ | █ | | | | | | |
| | Documentation for cases | | | | | | █ | █ | █ | | | | | | |
| 6 | Submission of Progress Report | | | | | | | | | █ | | | | | |
| 7 | Seminar 2 | | | | | | | | | | █ | | | | |
| 8 | Project Continues | | | | | | | | | | | | | | |
| | CFD Software Training | | | | | | | | █ | █ | | | | | |
| | Familiarizing with CFD Software | | | | | | | | | █ | █ | █ | █ | █ | |
| 9 | Submission of Interim Report | | | | | | | | | | | | | █ | |
| 10 | FYP1 Oral Presentation | | | | | | | | | | | | | | █ |

7.2 Gantt Chart of FYP II

| Num | FYP1 Activities | 1 | 2 | 3 | 4 | 5 | 6 | 7 | 8 | 9 | 10 | 11 | 12 | 13 | 14 |
|-----|---|---|---|---|---|---|---|---|---|---|----|----|----|----|----|
| 1 | Start simulation on case study | █ | █ | █ | | | | | | | | | | | |
| 2 | Submission of Progress Report 1 | | | | █ | | | | | | | | | | |
| 3 | Simulation in progress | | | █ | █ | █ | █ | | | | | | | | |
| 4 | Submission of Progress Report 2 | | | | | | | █ | | | | | | | |
| 5 | Seminar (compulsory) | | | | | | | | █ | █ | █ | █ | | | |
| 5 | Simulation result extraction and visualisation | | | | | | | █ | █ | █ | █ | | | | |
| 6 | Poster Exhibition | | | | | | | | | | █ | | | | |
| 7 | Submission of Dissertation (soft bound) | | | | | | | | | | | | █ | | |
| 8 | Oral Presentation | | | | | | | | | | | | | █ | |
| 9 | Submission of Project Dissertation (Hard Bound) | | | | | | | | | | | | | | █ |